Engineering Fracture Mechanics 77 (2010) 1101–1115

Contents lists available at ScienceDirect

Engineering Fracture Mechanics

journal homepage: www.elsevier.com/locate/engfracmech

Time-harmonic crack problems in functionally graded piezoelectric solids via BIEM

Petia Dineva [a], Dietmar Gross [b], Ralf Müller [c], Tsviatko Rangelov [d,*]

[a] Institute of Mechanics, Bulgarian Academy of Sciences, Sofia 1113, Bulgaria
[b] Division of Solid Mechanics, Technische Universität Darmstadt, 64289 Darmstadt, Germany
[c] Chair of Applied Mechanics, Department of Mechanical and Process Engineering, Technische Universität Kaiserslautern, 67653 Kaiserslautern, Germany
[d] Institute of Mathematics and Informatics, Bulgarian Academy of Sciences, Sofia 1113, Bulgaria

ARTICLE INFO

Article history:
Received 5 June 2009
Received in revised form 30 November 2009
Accepted 13 December 2009
Available online 21 December 2009

Keywords:
Functionally graded GaN material
In-plane cracks
Boundary element analysis
Stress intensity factor

ABSTRACT

In-plane crack analysis of functionally graded piezoelectric solids under time-harmonic loading is performed by using a non-hypersingular traction based boundary integral equation method (BIEM). The material parameters are assumed to vary quadratically with both spatial variables. A frequency dependent fundamental solution, as well as its derivatives and asymptotic expressions, is derived in closed-form by using an appropriate algebraic transformation for the displacement vector and the Radon transform. Numerical results for the stress intensity factors (SIFs) are discussed for different examples. The accuracy of the presented method is checked by comparison with available results from the literature. Investigated are the effects of the inhomogeneity parameters, the frequency of the applied electromechanical load and the geometry of the crack scenario on the K-factors.

1. Introduction

Piezoelectric functionally graded materials (FGMs) are composites with continuously varying properties that have significant advantages over discretely layered materials. The most used piezoelectric devices as bimorphs and monomorphs usually consist of two long and thin piezoelectric elements, which are bonded along their long faces by adhesive epoxy resin, and suitable covered with electrodes. The well-known drawback is that the bonding agent may crack during the fabrication process or in-service loading conditions. The advantage of using devices made of FGMs or its usage as a transit layer instead of the bonding agent is that failure from internal debonding or from stress peaks in conventional bimorphs can be avoided. The gradual variation of material properties in piezoelectric is quite effective to decrease the thermal and residual stresses and to increase the bonding strength and toughness. In principle, by controlling the material gradation during the manufacturing process, the desired electromechanical response may be attained. The special feature of graded spatial compositions provides some freedom in the design of novel smart structures.

On the other hand, FGMs are challenging regarding modeling and numerical simulation of their inhomogeneous structure. The mathematical background of models describing the mechanical behavior of these materials involves the solution of partial differential equations with spatially varying coefficients. The number of works devoted to dynamically loaded cracks in inhomogeneous piezoelectric materials is rather small. Most of them are focused on the anti-plane case, see Li and Weng [1], Wang and Zhang [2], Ma et al. [3,4], Rangelov et al. [5], Ding and Li [6], Chue and Ou [7], Keqiang et al. [8], Chen et al. [9]. The method used therein is mainly the singular integral equation method. There are only a few papers dealing

* Corresponding author. Tel.: +359 (0) 2979 2845; fax: +359 (0) 2971 3649.
E-mail address: rangelov@math.bas.bg (T. Rangelov).

0013-7944/$ - see front matter © 2010 Elsevier Ltd. All rights reserved.
doi:10.1016/j.engfracmech.2009.12.002

Nomenclature

a	inhomogeneity parameter (Section 2)
c	half crack length (Section 5.1)
C_{iJKl}	generalized stiffness tensor (Section 2)
C^0_{iJKl}	generalized stiffness tensor of the reference material (Section 2)
d	dimensionless magnitude (Section 5.2)
D_i	electric displacement's components (Section 2)
e_{ij}	piezoelectric coefficients (Section 2)
E_i	electric field's components (Section 2)
G	piezoelectric solid (Section 2)
$h(x)$	inhomogeneity function (Section 2)
K	K-factor, stress intensity factor (Section 1)
K_I	mode 1 stress intensity factor (Section 5.1, Eq. (15))
K_{II}	mode 2 stress intensity factor (Section 5.1, Eq. (15))
K_{IV}	mode 4 stress intensity factor (Section 5.1, Eq. (15))
K_D	K_{IV}, electric displacement intensity factor (Section 5.1)
K_E	electric field intensity factor (Section 5.1, Eq. (16))
S	boundary of the piezoelectric solid G (Section 2)
S_{cr}	crack's line (Section 2)
t_J	generalized traction's components (Section 2)
u_J	generalized displacement's components (Section 2)
u^*_{KM}	components of the fundamental solution of Eq. (8) (Section 3)
U^*_{KM}	components of the fundamental solution of Eq. (10) (Section 3)
l_j	length of the j-th boundary element (Section 5.2)
s_{Kl}	generalized strain (Section 2)
r	magnitude of the inhomogeneity gradient (Section 2)
α	direction of the inhomogeneity gradient (Section 2)
δ	Dirak's distribution (Section 3, Eq. (8))
δ_{JK}	Kroneker simbol (Section 3, Eq. (8))
Δu_J	generalized crack opening displacement(Section 4, Eq. (14))
ε_{ii}	dielectric coefficients (Section 2)
φ	orthotropy ratio (Section 5.2)
ϕ	electric potential (Section 2)
ω	frequency of the electromechanical loading (Section 2)
Ω	normalized frequency (Section 5.2)
ρ	mass density (Section 2, Eq. (1))
σ_{lJ}	generalized stress (Section 2)
σ^*_{lJM}	stress of the fundamental solution (Section 3)

Acronyms

BIEM	boundary integral equation method (Section 1)
BIE	boundary integral equation (Section 1)
BVP	boundary-value problem (Section 1)
COD	crack opening displacement (Section 4)
GaN	gallium nitrate (Section 1)
FGM	functionally graded material (Section 1)
SIF	stress intensity factor (Section 1)
2D	two-dimensional (Section 1)

with the respective in-plane case. The dynamic piezoelectric Mode-I problem is treated in Chen et al. [10] where the material properties are assumed to vary continuously only along one coordinate axis. Using the singular integral equation method the influence of the inhomogeneity on the K-factors for an impact loading is studied. In Chen and Liu [11] crack interaction is investigated based on the same method. The dynamic response of an exponentially graded piezoelectric finite plate containing a crack perpendicular to the free boundaries under the action of normal impact is considered in Ueda [12]. The same author in [13,14] studied the problem of a finite crack in a graded piezoelectric strip by using the singular integral equation method after applying integral transform technique. As an alternative numerical tool the meshless formulation in recent years has been successfully applied to homogeneous and inhomogeneous piezoelectric problems, see Sladek et al. [15–17]. In Sladek et al. [16] this method is used for the solution of central and edge crack problems in strips subjected to pure static mechanical and/or electrical loads. The same configurations under Heaviside impact loadings are solved in Sladek et al. [17] for impermeable and permeable cracks.

The BIEM has well-known advantages for the solution of linear problems in fracture mechanics. At the same time the direct application of the BIEM to crack problems leads to degeneration and then other computational techniques of this method are developed (see Chen and Hong [18], Aliabadi [19]), such as: (a) the multi-domain method [19], introducing artificial boundaries into the body by connecting the crack to the boundary in such a way so that each region contains a crack surface; (b) the non-hypersingular traction based BIEM derived by using the two-state conservation law of elastodynamic in its integral form [20]; (c) the dual boundary element method based on the dual integral equations in a general formulation which incorporates the displacement and traction BIEs, see Hong and Chen [18,21]. The application of the BIEM to dynamic problems in inhomogeneous piezoelectric solids meets serious difficulties because the method requires the fundamental solution for the corresponding FGM. In general, partial differential equations with variable coefficients do not possess explicit fundamental solutions that can easily be implemented in the existed BIEM software. This prevents the reduction of a boundary-value problem (BVP) to a system of boundary integral equations (BIE) which can be treated by standard numerical quadrature techniques. The key role of the fundamental solution in a BIEM formulation is to reduce a given BVP into a system of BIE by using the reciprocal theorem. For this reason the representation of the fundamental solutions in analytical form is so important. In elastodynamics, the following ways have been proposed to obtain BIEM solutions for inhomogeneous elastic continua: (i) Use of available fundamental solutions for homogeneous material, see Manolis and Shaw [22]. Here, by applying suitable algebraic transformations the partial differential equation with variable coefficients is reduced to one with constant coefficients. (ii) Use of the dual-reciprocity BIEM based on the fundamental solution for the homogeneous case, see Park and Ang [23] and Ang et al. [24]. Fundamental solutions for restricted cases of quadratic and exponential inhomogeneous piezoelectric material have been derived in Rangelov and Dineva [25] by using an appropriate algebraic transformation and the properties of the Radon transform.

The literature review shows that there exist only a few results for dynamic in-plane crack problems in inhomogeneous piezoelectric solids. To the authors best knowledge the 2D problem for a crack in a functionally graded piezoelectric solid under time-harmonic mechanical and electrical loading has not been solved up to now.

The aim of the present work is to develop a non-hypersingular traction BIEM for SIFs computation of in-plane cracked functionally graded piezoelectric materials based on the frequency dependent fundamental solution. The applicability of the method is demonstrated by numerical examples for the GaN piezoelectric material. This paper is an extension of our efforts in [5] where we consider anti-plane cracked piezoelectric solids. Both papers aim to show that stress concentration fields near the crack-tips in piezoelectric solids depend not only on different factors discussed separately in each of the two works, but also depend on the polarization phenomenon which is extremely significant in the areas of the smart structures and multifunctional materials.

The paper is organized as follows: The problem formulation for a cracked finite piezoelectric solid is given in Section 2. The fundamental solution for a quadratic type of inhomogeneity is described in Section 3. The non-hypersingular traction based BIEM is solved in Section 4. A series of numerical results for different examples is presented in Section 5, followed by a discussion and some conclusions in Section 6.

2. Formulation of the boundary-value problem

Consider the 2D problem of a finite inhomogeneous piezoelectric solid G with a smooth boundary S and an internal crack – an open arc S_{cr}, subjected to time-harmonic with a prescribed frequency ω electromechanical loading, see Fig. 1. Let the poling direction coincides with the x_3-axis of the coordinate system and assume plane-strain conditions in the x_1, x_3-plane. The mechanical and electrical loading is assumed to be such that the only non-zero field quantities are the displacement u_i, the stress σ_{ij}, the electric field E_i and the electric displacement D_i, where $i,j = 1,3$. In this case the governing equations in the absence of volume forces consist of the mechanical and electrical balance equations in the frequency domain

$$\sigma_{ij,i} + \rho\omega^2 u_j = 0, \quad D_{i,i} = 0, \tag{1}$$

the strain-displacement and electric field-potential relations

$$s_{ij} = \frac{1}{2}(u_{i,j} + u_{j,i}), \quad E_i = -\phi_{,i} \tag{2}$$

and the constitutive equations

$$\begin{aligned}
\sigma_{11} &= c_{11}u_{1,1} + c_{13}u_{3,3} + e_{31}\phi_{,1} \\
\sigma_{33} &= c_{13}u_{1,1} + c_{33}u_{3,3} + e_{33}\phi_{,3} \\
\sigma_{13} &= c_{44}u_{1,3} + c_{44}u_{3,1} + e_{15}\phi_{,3} \\
D_1 &= e_{15}u_{1,3} + e_{15}u_{3,1} - \varepsilon_{11}\phi_{,1} \\
D_3 &= e_{31}u_{1,1} + e_{33}u_{3,3} - \varepsilon_{33}\phi_{,3}
\end{aligned} \tag{3}$$

Here ϕ, s_{ij} and ρ are the electric potential, the strain tensor and the mass density, respectively. Subscript commas denote partial differentiation and the summation convention over repeated indices is invoked. The material tensor consists of the elastic stiffnesses $c_{11}, c_{33}, c_{44}, c_{13}$, the piezoelectric constants e_{31}, e_{33}, e_{15} and the dielectric constants $\varepsilon_{11}, \varepsilon_{33}$. Using the Voigt

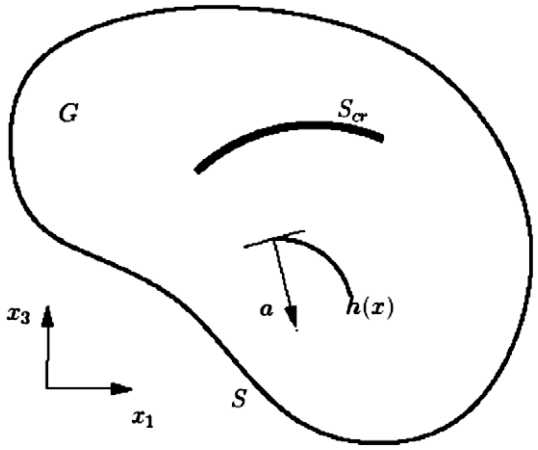

Fig. 1. Cracked inhomogeneous finite piezoelectric solid.

notation where $u_K = (u_1, u_3, \phi), s_{Kl} = (s_{11}, s_{33}, 2s_{13}, E_1, E_3), \sigma_{lK} = (\sigma_{11}, \sigma_{33}, \sigma_{13}, D_1, D_3), t_J = \sigma_{ij} n_i$ are the generalized displacement, strain, stress, traction and n_i is the outer normal vector to the boundary, respectively, Eqs. (1)–(3) can be written in the compact form

$$\sigma_{ij,i} + \rho_{JK}\omega^2 u_K = 0, \tag{4}$$

where

$$\sigma_{iJ} = C_{ijKl} u_{K,l} = C_{ijKl} s_{Kl} \quad \text{and} \quad \rho_{JK} = \begin{cases} \rho, & J, K = 1, 3, \\ 0, & J = 4 \text{ or } K = 4. \end{cases} \tag{5}$$

Here, the generalized stiffness tensor is given by

$$C = \begin{pmatrix} c & e \\ e' & -\varepsilon \end{pmatrix}, \quad c = \begin{pmatrix} c_{11} & c_{13} & 0 \\ c_{13} & c_{33} & 0 \\ 0 & 0 & c_{44} \end{pmatrix}, \quad e = \begin{pmatrix} 0 & e_{31} \\ 0 & e_{33} \\ e_{15} & 0 \end{pmatrix}, \quad \varepsilon = \begin{pmatrix} \varepsilon_{11} & 0 \\ 0 & \varepsilon_{33} \end{pmatrix}.$$

where e' is the transpose matrix to the matrix e. The matrices C and ε are assumed to be positive definite in order to ensure the thermodynamical based necessary condition of a stable piezoelectric material, see Dieulesaint and Royer [26].

We assume that the mass density and the material parameters vary in the same manner with $x = (x_1, x_3)$, i.e. there exists a function $h(x) = (a_1 x_1 + a_3 x_3 + 1)^2, h(x) > 0$ in G, such that $C_{ijKl}(x) = C^0_{ijKl} h(x)$ and $\rho_{JK}(x) = \rho^0_{JK} h(x)$. The constant vector $a = (a_1, a_3)$ is such that $\overline{G} \bigcap \{(x_1, x_3) : a_1 x_1 + a_3 x_3 + 1 = 0\} = \emptyset$. The main inhomogeneity parameter, the vector a can be written in polar coordinates as $a = (r\cos\alpha, r\sin\alpha)$, where $\alpha \in [0, \pi]$ and $r = \sqrt{a_1^2 + a_3^2}$ are the direction and the magnitude of the inhomogeneity gradient. Furthermore, regarding the reference material tensor, the following restrictions are assumed:

$$c^0_{13} = c^0_{44} \quad \text{and} \quad e^0_{31} = e^0_{15} \tag{6}$$

These equalities are approximately fulfilled for example for the piezoelectric material GaN, see Bykhovski et al. [27] and Levinshtein et al. [28].

The problem statement is completed by the boundary conditions. They are given on the outer boundary S by a prescribed displacement $\bar{u}_J$ on the part of the boundary S_u and a prescribed traction $\bar{t}_J$ on the complementary part $S_u, S = S_u \bigcup S_t$, $S_u \bigcap S_t = \emptyset$. The finite crack S_{cr} here is assumed to be impermeable and mechanical traction free:

$$u_J|_{S_u} = \bar{u}_J, \quad t_J|_{S_t} = \bar{t}_J, \quad t_J|_{S_{cr}} = 0, \tag{7}$$

but also other crack boundary conditions could have been used.

Our aim is to solve the BVP (4) and (7) via a validated BIEM. For this purpose, using an appropriate fundamental solution, the BVP must be formulated as an equivalent integrodifferential equation on the crack surface S_{cr} and the solid's surface S.

3. Inhomogeneity and fundamental solution

The fundamental solution of Eq. (4) is defined as solution of the equation

$$\sigma^*_{ijM,i} + \rho_{JK}\omega^2 u^*_{KM} = -\delta_{JM}\delta(x - \xi) \tag{8}$$

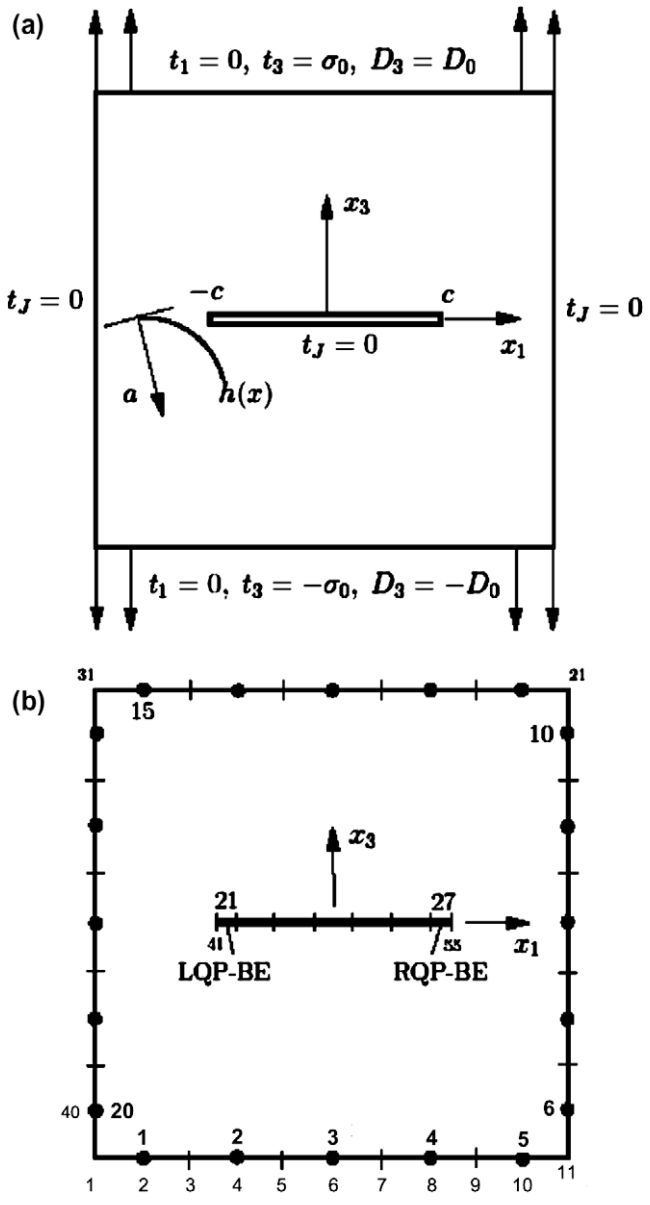

Fig. 2. Inhomogeneous rectangular plate (a), discretization (b).

where $\sigma^*_{ijM} = C_{ijKl}u^*_{KM,l}, x = (x_1, x_3), \xi = (\xi_1, \xi_3); \delta$ is Dirac's distribution and δ_{JM} the Kronecker symbol. The fundamental solution is derived in three steps, see Rangelov and Dineva [25]. First, by a suitable change of functions, Eq. (8) is transformed into an equation with constant coefficients. In the second step, Radon transform is applied. The system of differential equations then is decoupled via linear algebra tools. The third step is to apply the inverse Radon transform and to find the fundamental solution.

Applying the smooth transformation of u^*_{KM} in G as

$$u^*_{KM} = h^{-1/2}U^*_{KM} \tag{9}$$

Eq. (8) becomes an equation for U^*_{KM} with constant coefficients. Indeed,

$$\sigma^*_{ijM,i} + \rho_{JK}\omega^2 u^*_{KM} = h^{1/2}\{C^0_{ijKl}[U^*_{KM,il} + h^{-1/2}(h^{1/2}_{,i}U^*_{KM,l} - h^{1/2}_{,l}U^*_{KM,i} - h^{1/2}_{,il}U^*_{KM})] + \rho^0_{JK}\omega^2 U^*_{KM}\} = h^{1/2}[C^0_{ijKl}U^*_{KM,il} + \rho^0_{JK}\omega^2 U^*_{KM}]$$

since $h^{1/2}_{,il} = 0$ and due to restriction (6), $C^0_{ijKl}(h^{1/2}_{,i}U^*_{KM,l} - h^{1/2}_{,l}U^*_{KM,i}) = 0$ is satisfied. Dividing (8) by $h^{1/2}$ and having in mind that $h^{-1/2}(x)\delta(x,\xi) = h^{-1/2}(\xi)\delta(x,\xi)$ we obtain

$$[M_{JK}(\partial) + \Gamma_{JK}]U^*_{KM} = -h^{-1/2}(\xi)\delta_{JM}\delta(x-\xi), \quad (x,\xi) \in G \times G \tag{10}$$

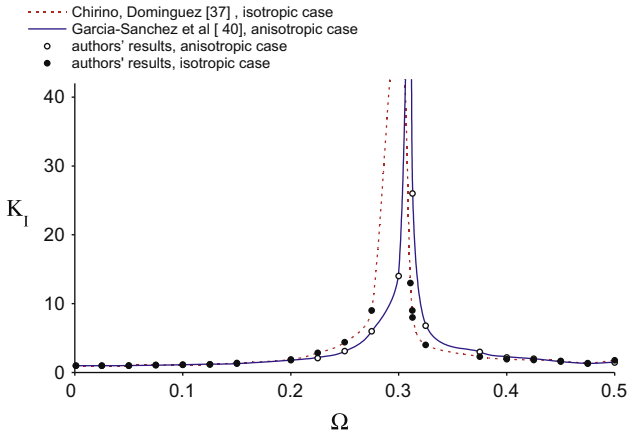

Fig. 3. Normalized K_I versus normalized frequency Ω for a center cracked isotropic/anisotropic homogeneous plate.

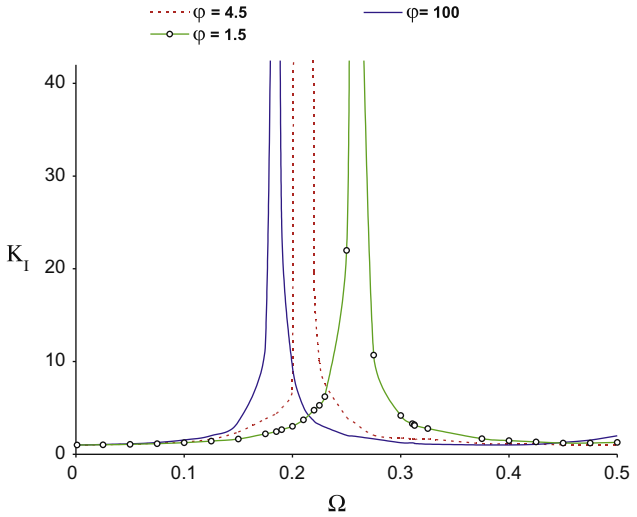

Fig. 4. Normalized K_I versus normalized frequency Ω for a center cracked anisotropic homogeneous Boron-epoxy I composite at different orthotropy ratios.

where $M_{JK}(\partial) = C^0_{iJKl}\partial_i\partial_l$, $\Gamma_{JK} = \rho^0_{JK}\omega^2$. Eq. (10) represents three systems of linear partial differential equations of second order with constant coefficients. Applying Radon transform, see Zayed [29], to both sides of Eq. (10), solving the obtained system of ordinary differential equations and applying the inverse Radon transform a fundamental solution of Eq. (8) in the form

$$u^*_{JK} = h^{-1/2}(\xi)h^{-1/2}(x)U^{*0}_{JK} \tag{11}$$

is derived where U^{*0}_{JK} is the fundamental solution for the homogeneous case, see Gross et al. [30]. The stress, associated to the fundamental solution, is

$$\sigma^*_{ijM} = C_{ijKl}[h^{-1/2}_{,l}(\xi)h^{-1/2}(x)U^{*0}_{KM} + h^{-1/2}(x)h^{-1/2}(\xi)U^{*0}_{KM,l}] \tag{12}$$

The representations (11) and (12) for the fundamental solution and the associated stress show their dependence on the mechanical properties of the reference material, on the location and distance between the source and observation point, on the frequency of the applied load and on the inhomogeneity function and it's derivatives. Using the properties of the sine and cosine integral functions for small arguments and the properties of the function h, the asymptotic behavior of (11) and (12) for $x \to \xi$ is given by

$$\begin{aligned} u^{*as}_{JK} &= h^{-1}(\xi)b_{JK}\ln|x-\xi|, \\ \sigma^{*as}_{ijM} &= h^{-1/2}(\xi)h_{,l}(\xi)p_{ijMl}\ln|x-\xi| + q_{ijM}\frac{1}{|x-\xi|} \end{aligned} \tag{13}$$

where b_{JK}, p_{ijMl} and q_{ijM} depend on the elastic, dielectric, piezoelectric constants and the density, but not on the frequency.

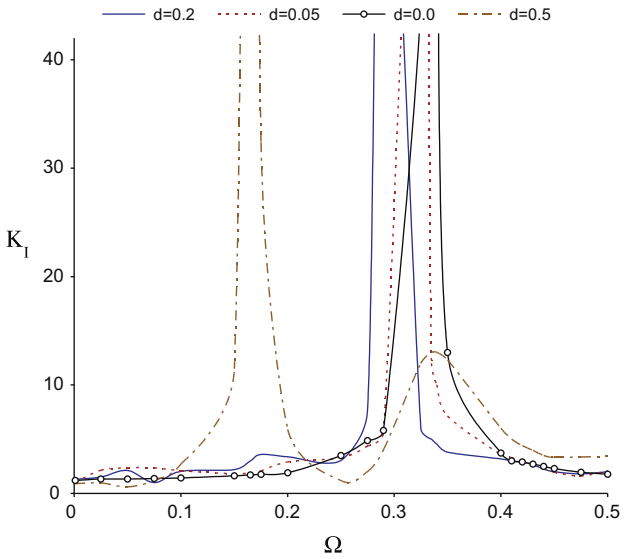

Fig. 5. Normalized K_I versus normalized frequency Ω for a center cracked inhomogeneous anisotropic plate. Material gradient direction $\alpha = \pi/2$.

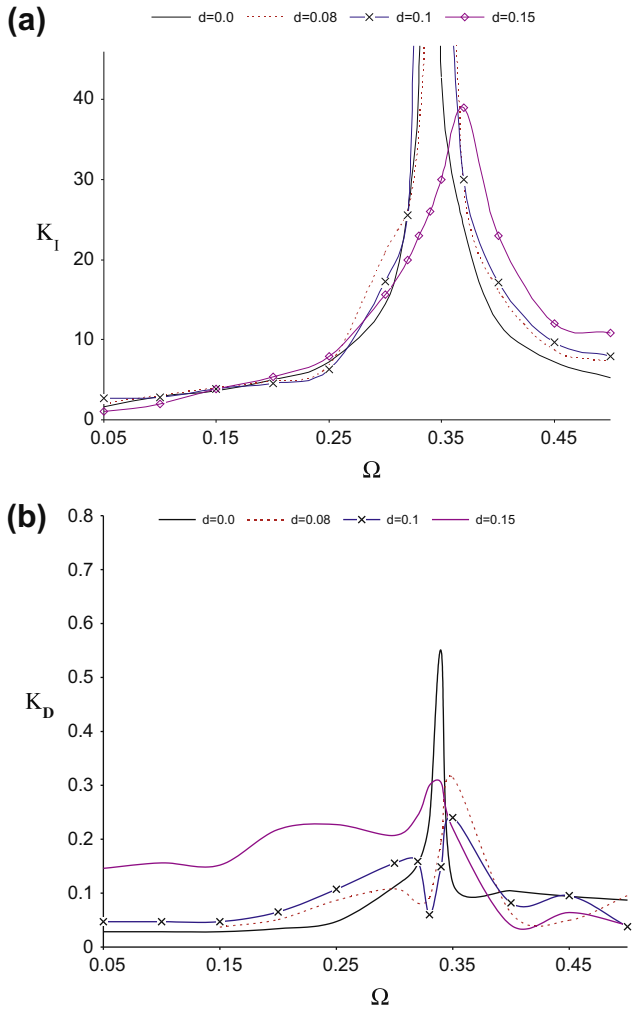

Fig. 6. Normalized SIFs versus normalized frequency Ω for a center cracked inhomogeneous piezoelectric plate. Material gradient direction $\alpha = \pi/2$. (a) K_I, (b) K_D.

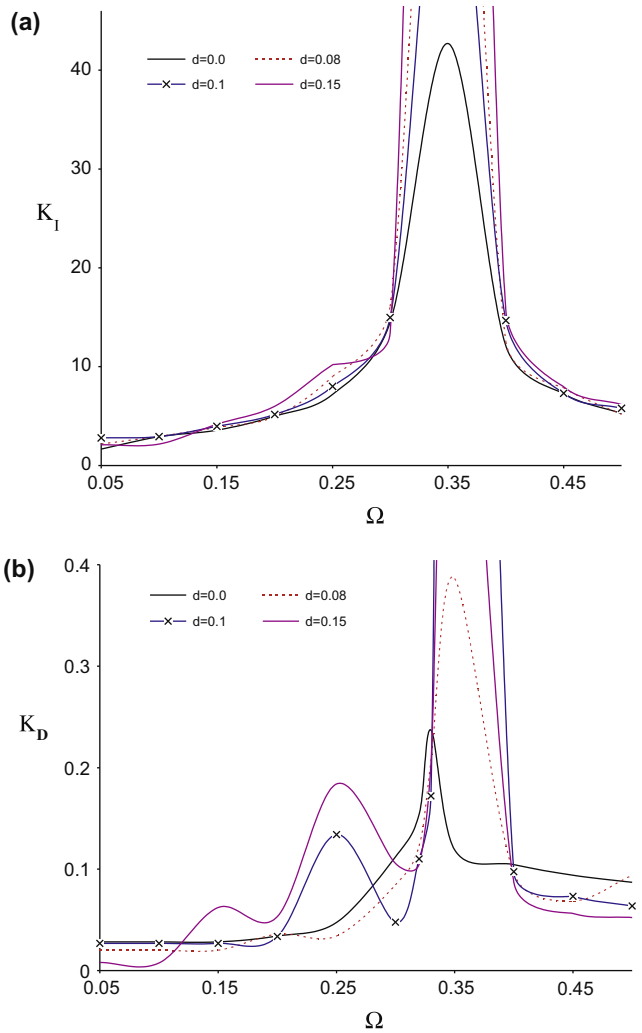

Fig. 7. Normalized SIFs versus normalized frequency Ω at the right crack-tip for a center cracked inhomogeneous piezoelectric plate. Material gradient direction $\alpha = \pi/9$. (a) K_I, (b) K_D.

4. Non-hypersingular traction BIEM

Following the method of Zhang and Gross [20] for homogeneous elastic isotropic materials, Wang and Zhang [2] and Gross et al. [31] for homogeneous piezoelectric materials, the non-hypersingular BIE formulation on the boundaries $S \bigcup S_{cr}$ is derived. For the considered linear BVP, Eqs. (4) and (7) the superposition principle is valid, see [32,33] and the displacement and traction are written as $u_J = u_J^0 + u_J^c, t_J = t_J^0 + t_J^c$. Here u_J^0, t_J^0 are the fields due to the external load on the boundary S of the crack free body, while the fields u_J^c, t_J^c are induced by the load $t_J^c = -t_J^0$ on the crack S_{cr} with zero boundary conditions on the boundary S. Using the representation formula for the generalized displacement gradients $u_{K,l}$ and taking the limit $x \to S \bigcup S_{cr}$ the following system of non-hypersingular traction BIEs for the posed problem is obtained:

$$
\begin{aligned}
\frac{1}{2}t_J^0(x) &= C_{iJKl}(x)n_i(x)\int_S [(\sigma^*_{\eta PK}(x,y)u^0_{P,\eta}(y) - \rho_{QP}\omega^2 u^*_{QK}(x,y)u^0_P(y))\delta_{\lambda l} - \sigma^*_{\lambda PK}(x,y)u^0_{P,l}(y)]n_\lambda dS \\
&\quad - C_{iJKl}(x)n_i(x)\int_S u^*_{PK,l}(x,y)t^0_P(y)dS, \quad x \in S, \\
t_J(x) &= C_{iJKl}(x)n_i(x)\int_{S^+_{cr}} [(\sigma^*_{\eta PK}(x,y)\Delta u^c_{P,\eta}(y) - \rho_{QP}\omega^2 u^*_{QK}(x,y)\Delta u^c_P(y))\delta_{\lambda l} - \sigma^*_{\lambda PK}(x,y)\Delta u^c_{P,l}(y)]n_\lambda(y)dS_{cr} \\
&\quad + C_{iJKl}(x)n_i(x)\int_S [(\sigma^*_{\eta PK}(x,y)u^c_{P,\eta}(y) - \rho_{QP}\omega^2 u^*_{QK}(x,y)u^c_P(y))\delta_{\lambda l} - \sigma^*_{\lambda PK}(x,y)u^c_{P,l}(y)]n_\lambda dS \\
&\quad - C_{iJKl}(x)n_i(x)\int_S u^*_{PK,l}(x,y)t^c_P(y)dS, \quad x \in S \cup S_{cr}
\end{aligned}
\tag{14}
$$

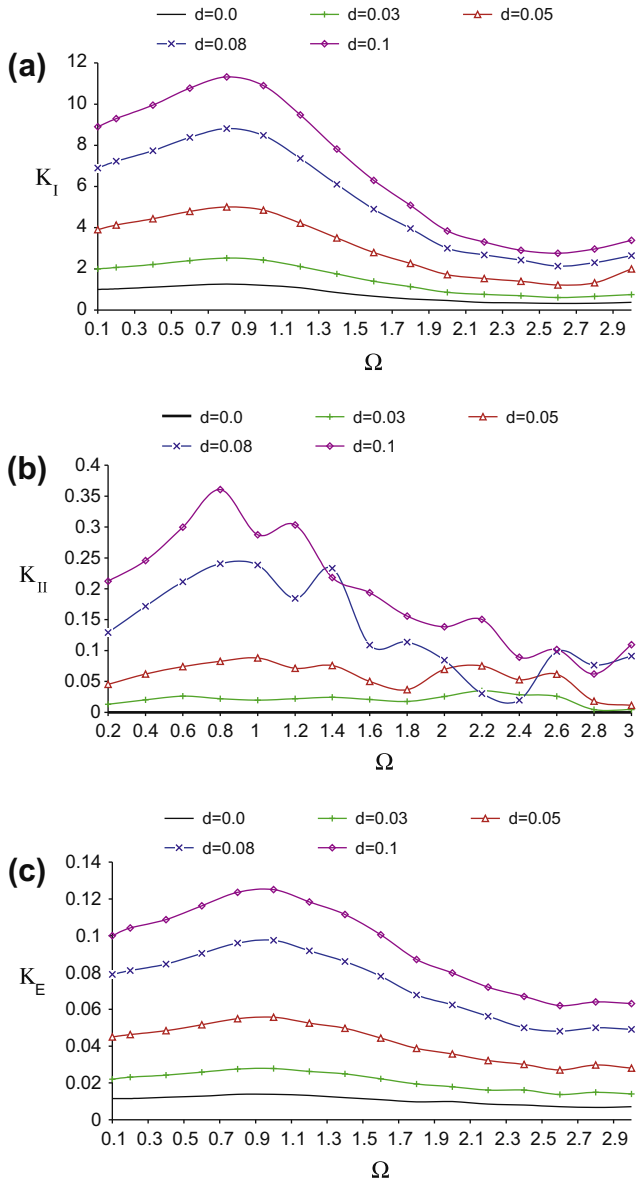

Fig. 8. Normalized SIFs versus normalized frequency Ω at the right crack-tip for a piezoelectric inhomogeneous plate. (a) K_I, (b) K_{II}, (c) K_E.

where

$$t_J = \begin{cases} t_J^c/2 \text{ on } S \\ -t_J^0 \text{ on } S_{cr} \end{cases}$$

and $\Delta u_J^c = u_J^c|_{S_{cr}^+} - u_J^c|_{S_{cr}^-}$ is the generalized crack opening displacement (COD). Furthermore, $x = (x_1, x_3)$ and $y = (y_1, y_3)$ denote the position vector of the observation point and source point, respectively. Eq. (14) constitute an system of integrodifferential equations for the unknowns Δu_J^c on S_{cr} and u_J^0, u_J^c, t_J^c on S. From its solution the generalized displacement u_J and traction t_J at each internal point can be determined by using the corresponding representation formulae.

5. Numerical results

5.1. Solution procedure

The solution procedure follows the numerical algorithm developed and validated in Gross et al. [31] for the equivalent homogeneous piezoelectric problem. The boundaries S and S_{cr} are discretized by quadratic shape functions away from the

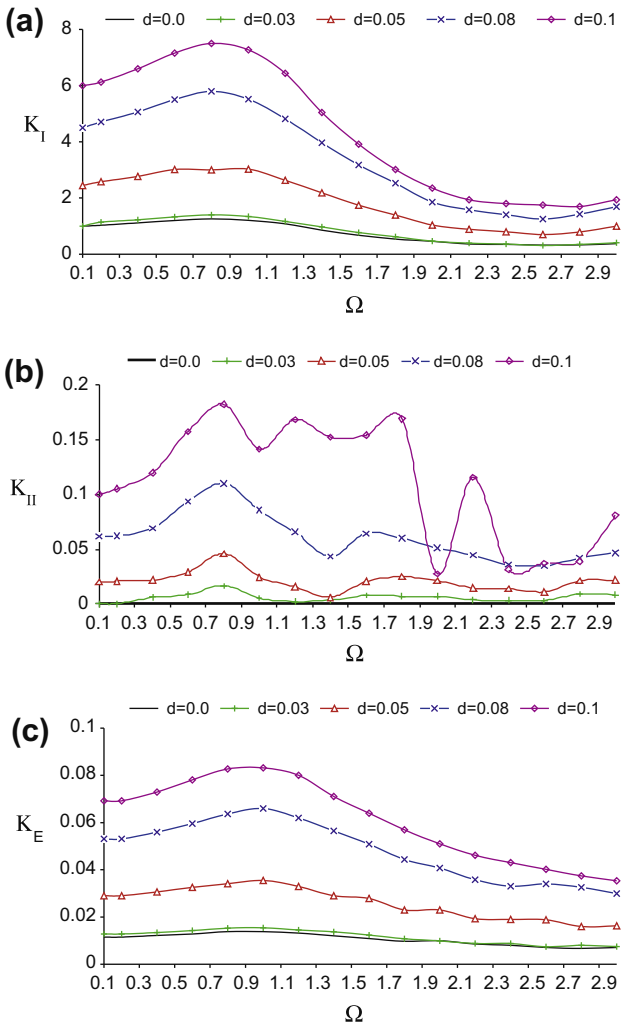

Fig. 9. Normalized SIFs versus normalized frequency Ω at the right crack-tip of a crack S_{cr} in piezoelectric inhomogeneous plane under normal time-harmonic uniform tension. (a) K_I, (b) K_{II}, (c) K_E. Inhomogeneity direction is $\alpha = \pi/4$.

crack-tip and special crack-tip quarter-point element near the crack-tip to model the correct asymptotic behavior of the displacement and traction. Applying the shifted point scheme, the singular integrals converge in Cauchy Principle Value sense, since the smoothness requirements $\Delta u_J \in C^{1+\alpha}(S_{cr}), u_J \in C^{1+\alpha}(S)$ and $t_J \in C^{\alpha}(S), \alpha < 1$ in the approximation are fulfilled, see Rangelov et al. [34].The regular integrals are computed employing Gaussian quadrature for one-dimensional integrals and Monte Carlo integration for two-dimensional integrals. All singular integrals are solved analytically in **a** small neighborhood of the observation point, utilizing the asymptotics of the fundamental solution for a small argument.

After the discretization procedure an algebraic system of equations is obtained and numerically solved. For this purpose, a FORTRAN code has been developed. Knowing the tractions, the generalized dynamic SIFs at the tips are calculated, see Suo et al. [35]. For example, in case of a straight crack along the interval $(-c, c)$ on the x_1-axis, the respective formulae are given by

$$\begin{aligned} K_I &= \lim_{x_1 \to \pm c} t_3 \sqrt{2\pi(x_1 \mp c)}, \\ K_{II} &= \lim_{x_1 \to \pm c} t_1 \sqrt{2\pi(x_1 \mp c)}, \\ K_{IV} &= \lim_{x_1 \to \pm c} t_4 \sqrt{2\pi(x_1 \mp c)}, \end{aligned} \tag{15}$$

where t_J is the generalized traction at the point $(x_1, 0)$ close to the crack-tip. Regarding the electrical SIFs, the electric field SIF K_E is given by

$$K_E = \lim_{x_1 \to \pm c} E_3 \sqrt{2\pi(x_1 \mp c)}, \quad E_3 = (c_{33}t_4 - e_{33}t_3)(e_{33}c_{33} + e_{33}^2)^{-1} \tag{16}$$

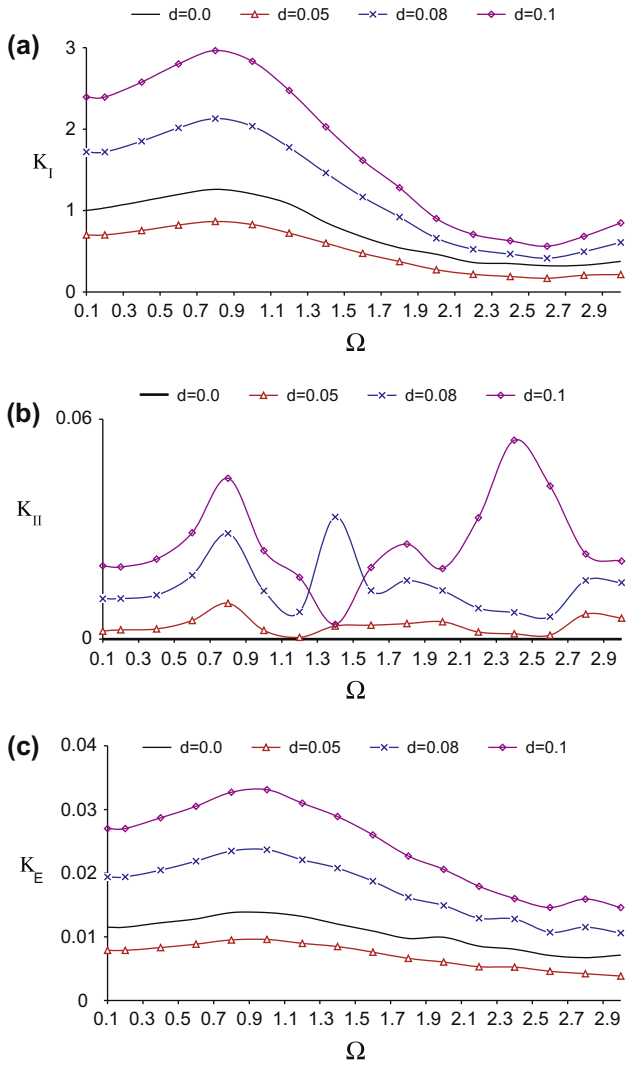

Fig. 10. Normalized SIFs versus normalized frequency Ω at the right crack-tip of a crack S_{cr} in piezoelectric inhomogeneous plane under normal time-harmonic uniform tension. (a) K_I, (b) K_{II}, (c) K_E. Inhomogeneity direction is $\alpha = \pi/9$.

and the electric displacement SIF $K_D = K_{IV}$ can also be determined. Eqs. (15) and (16) are based on the fact that the stresses and electric displacements at the crack-tip in functionally graded materials still exhibit a square-root singularity, see Kondratiev [36].

5.2. Results

The numerical study aims to illustrate the sensitivity of the mechanical and electrical SIFs on the frequency of the applied electromechanical load, on the direction and magnitude of the material gradient and on the geometry of the crack configuration.

In all examples a straight crack of length $2c = 5$ mm is considered which is discretized by 7 boundary elements (BE), see Fig. 2b. The numerical studies showed that this number is sufficient to achieve a satisfying accuracy within the considered frequency range. The first and the last element are quarter-point quadratic BE while the remaining elements are ordinary quadratic BE. Their lengths have been chosen as $l_1 = l_7 = 0.375$ mm, $l_2 = l_6 = 0.5$ mm, $l_3 = l_5 = 1.0$ mm, $l_4 = 1.25$ mm. As reference piezoelectric material GaN (Gallium Nitride) is taken with the following properties (see Bykhovski et al. [27] and Levinshtein et al. [28]): $c^0_{11} = 39.0 \times 10^{10}\ \mathrm{N/m^2}; c^0_{13} = c^0_{44} = 10.6 \times 10^{10}\ \mathrm{N/m^2}; c^0_{33} = 39.8 \times 10^{10}\ \mathrm{N/m^2}; e^0_{31} = e^0_{15} = -0.3\ \mathrm{C/m^2}, e^0_{33} = 0.65\ \mathrm{C/m^2}$, $\varepsilon^0_{11} = 0.8407 \times 10^{-10}\ \mathrm{C/Vm}, \varepsilon^0_{33} = 0.9204 \times 10^{-10}\ \mathrm{C/Vm}, \rho_0 = 6.5 \times 10^3\ \mathrm{kg/m^3}$.

The crack is centered in a rectangular plate with the dimensions 20 mm $\times$ 40 mm which is loaded by an uniform time-harmonic electromechanical tension along the x_3-axis at the opposite sides with amplitudes $\sigma_0 = 400 \times 10^6\ \mathrm{N/m^2}$ and $D_0 = 0.1\ \mathrm{C/m^2}$, see Fig. 2a and b. A normalized frequency is introduced through $\Omega = c\omega\sqrt{\rho_0/c^0_{44}}$, where $\omega[1/s]$ is the angular

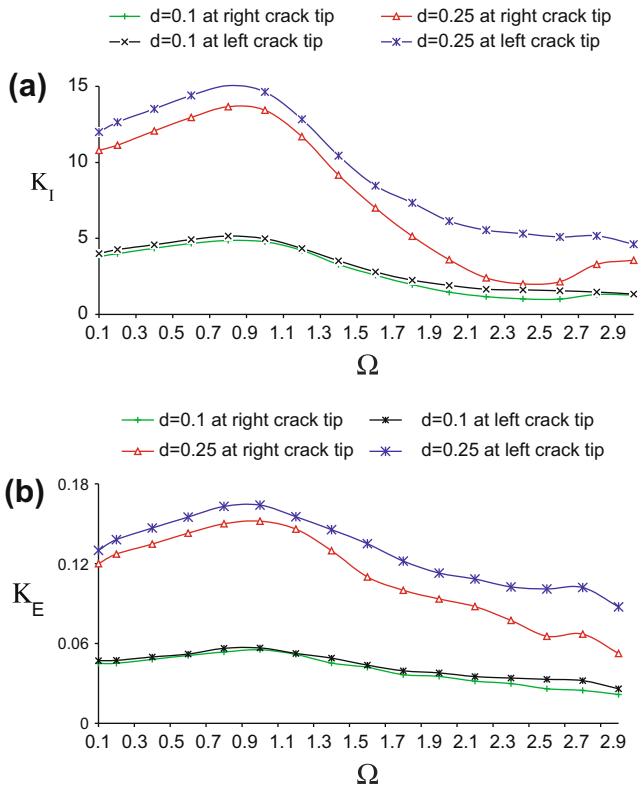

Fig. 11. Normalized SIFs versus normalized frequency Ω at the right and at the left crack-tips of a crack S_{cr} in a piezoelectric inhomogeneous plane under normal time-harmonic uniform tension. (a) K_I, (b) K_E. Inhomogeneity direction is $\alpha = \pi/6$.

frequency. The mechanical SIFs K_I and K_{II} are normalized by $\sigma_0\sqrt{\pi c}$, while the electrical SIF K_D is normalized by $D_0\sqrt{\pi c}$, and the electric field SIF K_E is normalized by $|\sigma_0|\sqrt{\pi c}/e_{33}$. A total number of 20 quadratic BE on the external boundary S have been used, see Fig. 2b.

A detailed validation study of the proposed numerical scheme for the homogeneous crack problem in an infinite region are presented in Gross et al. [30,31] and therefore is omitted here. For all examples the authors' BIEM solutions showed a very good agreement with the available results of Chirino and Dominguez [37], Ohyoshi [38] and Shindo and Ozawa [39].

For cracks in finite piezoelectric regions under time-harmonic loading no results, but the own authors' results in Gross et al. [31] are available up to now. However, a solution for a cracked anisotropic rectangular plate under time-harmonic load has been published by Garcia-Sanchez et al. [40]. Fig. 3 shows a comparison of the authors BIEM results: (a) with results of Chirino and Dominguez [37] for a homogeneous elastic isotropic material and (b) with results of Garcia-Sanchez et al. [40] for a homogeneous elastic anisotropic Boron-epoxy (type I) composite with the following properties: Young's moduli $E_1 = 224.06$ GPa,$E_3 = 12.69$ GPa, shear modulus $G_{13} = 4.43$ GPa and Poisson's ratio $\nu_{13} = 0.256$. It is observed a peak for the normalized frequency around 0.3 which is considered as a resonance value of the SIF. The existence of this resonance effect is described and discussed by several authors as for the isotropic cracked domains, see [37], so for the anisotropic cracked domains, see [40]. As can be seen, the results are in excellent agreement, although very different computational techniques are used in [37,40] and in the present investigation. To the author's knowledge there are no available results for SIF computation for finite cracked piezoelectric solids with quadratic inhomogeneity subjected to in-plane time-harmonic mechanical and electrical load. Due to this reason the validation is based on the comparison of the author's BIEM results with the results of other authors for the homogeneous case. Using the developed program code for inhomogeneous case and replacing the inhomogeneity function $h(x)$ with 1 we show the validation.

For the same homogeneous material, Fig. 4 shows BIEM results revealing the influence of the orthotropy ratio $\varphi = E_1/E_3$ on the SIFs. Here, the shear modulus has been defined as $G_{13} = E_1/(\varphi + 2\nu_{13} + 1)$, see Garcia-Sanchez et al. [41]. Fig. 4 shows that with increasing φ the resonance peak is shifted to lower frequencies and this effect is the same as those shown in [40].

Following Zhang et al. [32,42] the dimensionless magnitude $d = r.c$ and the direction α of the inhomogeneity gradient are defined, where the magnitude of the inhomogeneity gradient r is defined in Section 2 and c is the half-length of the crack. In Figs. 5–11 the inhomogeneity effects are evaluated with respect to d and α. First, by setting the piezoelectric constants of GaN to zero, the purely elastic anisotropic case is studied. For an inhomogeneity direction perpendicular to the crack, Fig. 5 shows the normalized K_I versus frequency Ω for different inhomogeneity magnitude d. With increasing d the resonance peak is shifted to lower frequencies. All further results are devoted to inhomogeneous piezoelectric materials.

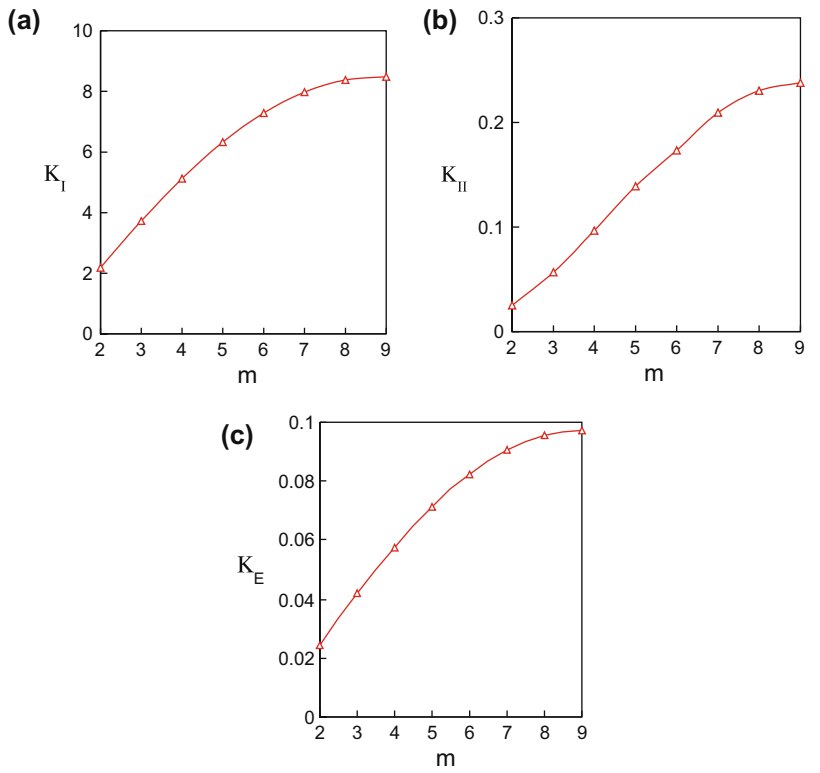

Fig. 12. Normalized SIFs K_I, K_{II}, K_E at the left crack-tip of a crack in inhomogeneous plane subjected to normal time-harmonic uniform tension versus the angle $m = k\frac{\pi}{18}, k = 2, \ldots, 9$ of the material gradient direction at normalized frequency $\Omega = 1$ and magnitude $d = 0.08$.

In Figs. 6 and 7a and b the SIFs at the right crack tip for different inhomogeneity magnitudes d and two different inhomogeneity directions ($\alpha = \pi/2$ and $\alpha = \pi/9$) are plotted. The following observations can be made: (a) Generally, the inhomogeneity effect is clearly visible. (b) The inhomogeneity effect is more pronounced for the electrical SIFs. (c) The FGM with $d = 0.15$ reduces the resonance amplitude, see Fig. 6a due to the material inhomogeneity. (d) A mode K_{II} factor appears under periodic uniaxial tension on account of the non-symmetry if the inhomogeneity direction is not perpendicular to the crack plane. This effect has been investigated for general FGMs recently by Zhang et al. [32,42] and Dineva et al. [43]. It will also be shown in the following examples where the external boundary has a minor influence on the complex wave field inside the solid and the inhomogeneity effects can be demonstrated more clear.

In the following examples, in order to decrease the disturbing wave reflection at the external boundary and to compare the present results with those for a finite crack in an infinite plane, the edge-length W of the square plate with the crack is taken sufficiently large, say $W = 7c$, as in Sladek et al. [44]. Fig. 8 demonstrates the influence of the magnitude of the material gradient d on K_I, K_{II} and K_E in the case the material properties vary normal to the crack line, i.e. the direction of the material gradient is $\alpha = \pi/2$. Figs. 9 and 10 show the same quantities but now for the inhomogeneity directions $\alpha = \pi/4$ and $\alpha = \pi/9$, respectively. In Fig. 11, for the inhomogeneity direction $\alpha = \pi/6$ and two different d, the K-factors at the right and the left crack tip are compared. It can be seen that, as could be expected, the difference between K factors at left and right crack-tips increase with increasing inhomogeneity magnitude d.

Finally, in Fig. 12 the K-factors for the left crack-tip are depicted in dependence of the gradient direction $\alpha \in [\pi/9, \pi/2]$ at the fixed frequency $\Omega = 1$ and gradient parameter $d = 0.08$. For these parameters, the highest SIFs are obtained when the direction of the material gradient is perpendicular to the crack. It shall be mentioned that this result cannot be generalized.

The numerical study clearly shows that the inhomogeneity has a strong influence on the SIFs, i.e. the dynamic stress concentration at the crack-tips. Because the dynamic crack tip field is a complex result of the influence of the different parameters like geometry, loading, electromechanical coupling, anisotropy strength, inhomogeneity strength and direction, the picture is not as clear as in the simple uncoupled static case. The results demonstrate that the SIFs are sensitive to the direction and magnitude of the material inhomogeneity, depend on the frequency of the applied load and on the relation between the magnitude of the gradient parameter and the crack size. The comparison of the results in Figs. 6 and 7 with those in Figs. 9–11 reveals the role of the reflected waves from the external boundaries of the finite piezoelectric solid and the influence of the geometry of the crack scenario on the obtained dynamic stress concentration field. It is important to note that K_{II} factor is not zero in the inhomogeneous case under pure tension in contrast to the homogeneous case.

6. Conclusion

Presented is an analytical methodology that derives the fundamental solutions for wave equations of a specific class of inhomogeneous piezoelectric materials with quadratic variation of the material characteristics. The non-hypersingular traction based BIE formulation of the dynamic problem for a cracked finite inhomogeneous solid subjected to in-plane mechanical and/or in-plane electrical load is presented. Using the derived fundamental solutions and accurate numerical procedure, an efficient BIEM software is developed and validated. Numerical examples for SIF computation in cracked piezoelectric functionally graded GaN materials and solids subjected to in-plane time-harmonic electromechanical loads are presented. Conclusion from the simulations is that the coupled crack-tip field is sensitive to the magnitude and direction of the material inhomogeneity gradient, to the frequency of the applied dynamic load, to the crack geometry and to the electromechanical coupling. Finally, although the results obtained herein are for a restricted type of inhomogeneity, the proposed methodology might be applicable for the solution of problems in non-destructive material testing and material science.

Acknowledgement

The authors acknowledge the support of the DFG under the Grant number GZ: 436 BUL 113/150/0-1.

References

[1] Li C, Weng G. Antiplane crack problem in functionally graded piezoelectric materials. J Appl Mech – T ASME 2002;69:481–8.
[2] Wang C-Y, Zhang Ch. 2D and 3D dynamic Green's functions and time-domain BIE formulations for piezoelectric solids. Engng Anal Bound Elem 2005;29:454–65.
[3] Ma L, Wu LZ, Zhou ZG, Guo LC, Shi LP. Scattering of harmonic anti-plane shear waves by two collinear cracks in functionally graded piezoelectric materials. Eur J Mech A – Solid 2004;23:633–43.
[4] Ma L, Wu LZ, Zhou ZG, Guo LC. Scattering of the harmonic anti-plane share waves by a crack in functionally graded piezoelectric materials. Compos Struct 2005;69:436–41.
[5] Rangelov T, Dineva P, Gross D. Effect of material inhomogeneity on the dynamic behavior of cracked piezoelectric solids: a BIEM approach. ZAMM – Z Angew Math Mech 2008;88:86–99.
[6] Ding SH, Li X. Periodic cracks in functionally graded piezoelectric layer bonded to a piezoelectric half-plane. Theor Appl Fract Mech 2008;49(3):313–20.
[7] Chue CH, Ou YL. Mode III crack problems for two bonded functionally graded piezoelectric materials. Int J Solids Struct 2005;42:3321–37.
[8] Keqiang H, Zheng Z, Bo J. Electroelastic intensification near anti-plane crack in a functionally gradient piezoelectric ceramic strip. Acta Mech Solida Sin 2003;16(3):197–204.
[9] Chen J, Liu ZX, Zou ZZ. The central crack problem for a functionally graded piezoelectric strip. Int J Fract 2003;121:81–94.
[10] Chen J, Liu ZX, Zou ZZ. Electromechanical impact of a functionally graded piezoelectric medium. Theor Appl Fract Mech 2003;39:47–60.
[11] Chen J, Liu ZX. On the dynamic behavior of a functionally graded piezoelectric strip with periodic cracks vertical to the boundary. Int J Solids Struct 2005;42:3133–46.
[12] Ueda S. Impact response of a functionally graded piezoelectric plate with a vertical crack. Theor Appl Fract Mech 2005;44:329–42.
[13] Ueda S. Crack in functionally graded piezoelectric strip bonded to elastic surface layers under electromechanical loading. Theor Appl Fract Mech 2003;40:325–36.
[14] Ueda S. Electromechanical response of a center crack in a functionally graded piezoelectric strip. Smart Mater Struct 2005;14:1133–8.
[15] Sladek J, Sladek V, Zhang Ch, Garcia-Sanchez F, Wunsche M. Meshless local Petrov-Galerkin method for plane piezoelectricity. CMC: Comput Mater Continua 2006;4:109–18.
[16] Sladek J, Sladec V, Zhang Ch, Solek P, Starek L. Fracture analysis in continuously non-homogeneous piezoelectric solids by the MLPG. Comput Methods Engng Sci 2007;19(3):247–62.
[17] Sladek J, Sladek V, Zhang Ch. A local integral equation method for dynamic analysis in functionally graded piezoelectric materials. In: Minutoto V, Aliabadi MH, editors. Advances in boundary element technique VIII. United Kingdom: EC Ltd.; 2007. p. 141–8.
[18] Chen JT, Hong H-K. Review of dual boundary element methods with emphasis on hyper-singular integrals and divergent series. Appl Mech Rev ASME 1999;52(1):17–33.
[19] Aliabadi MH. A new generation of boundary element methods in fracture mechanics. Int J Fract 1997;86:91–125.
[20] Zhang Ch, Gross D. On wave propagation in elastic solids with cracks. Southampton: Comp Mech Publ; 1998.
[21] Hong H-K, Chen JT. Derivations of Integral Equations of Elasticity. J Engng Mech – ASCE 1988;114(6):1028–44.
[22] Manolis G, Shaw R. Green's function for a vector wave equation in a mildly heterogeneous continuum. Wave Motion 1996;24:59–83.
[23] Park S, Ang W. A complex variable boundary element method for an elliptic partial differential equation with variable coefficients. Commun Numer Meth Engng 2000;16:697–703.
[24] Ang W, Clements D, Vahdati N. A dual-reciprocity boundary element method for a class of elliptic boundary value problems for non-homogeneous anisotropic media. Engng Anal Bound Elem 2003;27:49–55.
[25] Rangelov T, Dineva P. Dynamic behaviour of a cracked inhomogeneous piezoelectric solid. In-plan case. CR Acad Sci Bulg 2007;60(2):141–8.
[26] Dieulesaint E, Royer D. Elastic wave in solids. New York: John Wiley; 1974.
[27] Bykhovski AD, Gelmond BL, Shur MS. Elastic strain relaxation and piezoeffect in GaN-AIN, GaN-AlGaN and GaN-InGaN superlattices. J Appl Phys 1997;81(9):6332–8.
[28] Levinshtein ME, Rumyantsev SL, Shur MS. Properties of advanced semiconductor materials GaN, AIN, InN, BN and SiGe. London: John Wiley and Sons; 2001.
[29] Zayed A. Handbook of generalized function transformations. Boca Raton, Florida: CRC Press; 1996.
[30] Gross D, Rangelov T, Dineva P. 2D Wave scattering by a crack in a piezoelectric plane using traction BIEM. J Struct Integrity Durability 2005;1(1):35–47.
[31] Gross D, Dineva P, Rangelov T. BIEM solution of piezoelectric cracked finite solids under time-harmonic loading. Engng Anal Bound Elem 2007;31:152–62.
[32] Zhang C, Sladek J, Sladek V. Numerical analysis of cracked functionally graded materials. Key Engng Mater 2003;251, 252:463–71.
[33] Wang BL, Han JC, Du SY. Dynamic response for non-homogeneous piezoelectric medium with multiple cracks. Engng Fract Mech 1998;61:607–17.
[34] Rangelov T, Dineva P, Gross D. A hyper-singular traction boundary integral equation method for stress intensity factor computation in a finite cracked body. Engng Anal Bound Elem 2003;27:9–21.
[35] Suo Z, Kuo C, Barnett D, Willis J. Fracture mechanics for piezoelectric ceramics. J Mech Phys Solids 1992;40:739–65.
[36] Kondratiev V. Boundary problems for elliptic equarions in domain with conical and angular points. Proc Moscow Math Soc 1967;16:227–313.
[37] Chirino F, Dominguez J. Dynamic analysis of cracks using BEM. Engng Fract Mech 1989;34:1051–61.
[38] Ohyoshi T. Effect of orthotropy on singular stresses for a finite crack. J Appl Mech – T ASME 1973;40:491–7.

[39] Shindo Y, Ozawa E. Dynamic analysis of a cracked piezoelectric material. In: Hsieh RKT, editor. Mechanical modeling of new electromagnetic materials. Elsevier; 1990. p. 297–304.
[40] Garcia-Sanchez F, Saez A, Dominguez J. Two-dimensional time-harmonic BEM for cracked anisotropic solids. Engng Anal Bound Elem 2006;30:88–99.
[41] Garcia-Sanchez F, Saez A, Dominguez J. Traction boundary elements for cracks in anisotropic solids. Engng Anal Bound Elem 2004;28:667–76.
[42] Zhang C, Sladek J, Sladek V. Crack analysis in unidirectionally and bidimensionally functionally graded materials. Int J Fract 2004;129:385–406.
[43] Dineva P, Rangelov T, Manolis G. Elastic wave propagation in a class of cracked, functionally graded materials by BIEM. Comput Mech 2007;39:293–308.
[44] Sladek J, Sladek V, Zhang Ch. A meshless local boundary integral equation method for dynamic anti-plane shear crack problem in functionally graded materials. Engng Anal Bound Elem 2005;29:334–42.